Tissue-resident NK cells support survival in pancreatic cancer through promotion of cDC1-CD8T activity.

Running title

Radiotherapy and CCR5i/αPD1 Immunotherapy induce trNK cells and PDAC tumor control.

Authors

Simei Go[1], Constantinos Demetriou[1], Sophie Hughes[1], Simone Lanfredini[1], Giampiero Valenzano[1], Helen Ferry[2], Edward Arbe-Barnes[3], Shivan Sivakumar[1], Rachael Bashford-Rogers[4], Mark R. Middleton[1,2,5], Somnath Mukherjee[5], Jennifer Morton[6,7], Keaton Jones[8], Eric O'Neill[1]

Affiliations

[1]Department of Oncology, University of Oxford; Oxford, UK

[2]NIHR Oxford Biomedical Research Centre, Oxford University Hospitals.

[3]University of Oxford Medical School, OX3 9DU Oxford, UK

[4]Department of Biochemistry, University of Oxford, OX1 3QU Oxford, UK

[5]Oxford University Hospitals NHS Foundation Trust, Oxford, UK

[6]CRUK Beatson Institute, Garscube Estate, Switchback Road, Glasgow, G61 1BD, UK

[7]School of Cancer Sciences, University of Glasgow, Garscube Estate, Glasgow, G61 1QH, UK

[8]Nuffield Department of Surgical Sciences, University of Oxford; Oxford, UK

Contact information

Eric O'Neill

Department of Oncology

University of Oxford

Old Road Campus Research Building

Roosevelt Drive

Oxford

OX3 7DQ

eric.oneill@oncology.ox.ac.uk

Abstract

The immunosuppressive microenvironment in PDAC prevents tumor control but strategies to restore anti-cancer immunology, by increasing CD8 T cell activity, have not been successful. Here we demonstrate how inducing localized physical damage using ionizing radiation (IR) unmasks the benefit of immunotherapy by increasing tissue-resident NK (trNK) cells that support CD8 T activity. Our data confirms that targeting mouse orthotopic PDAC tumors with IR together with CCR5 inhibition and PD1 blockade reduces E-cadherin positive tumor cells by recruiting a hypofunctional NKG2C^{-ve} NK population that supports CD8 T cell involvement. We show an equivalent population in human PDAC cohorts that represents an adaptive-like immunomodulatory trNK-cell that similarly supports CD8 T cell levels in a cDC1-dependent manner. Importantly, a trNK signature associates with survival in PDAC and solid malignancies revealing a potential beneficial role for trNK in improving adaptive anti-tumor responses and supporting CCR5i/αPD1 and IR-induced damage as a novel therapeutic approach.

Introduction

Over the past decade, immune checkpoint inhibitors have shown significant success in the treatment of various solid malignancies. Treatment of pancreatic cancer using immunotherapy alone or in combination with radiotherapy or chemotherapy has unfortunately seen limited clinical success over either modality alone(Bockorny et al., 2020; Doi et al., 2019; Royal et al., 2010; Weiss et al., 2018; Weiss et al., 2017) (Mohindra et al., 2015). This is likely due to several tumor microenvironmental factors, including the dense stroma that supports an immunosuppressive environment while also obstructing the infiltration of cytotoxic immune cells(Mills et al., 2022; Piper et al., 2023). Novel strategies comprising dual targeting of PD-1/IL-2Rβγ with radiotherapy are beginning to indicate that potential benefits may require a coordinated alteration in the suppressive microenvironment involving loss of regulatory T cells (Tregs) and increased natural killer (NK) cell infiltration, in addition to simply increasing CD8 T infiltration(Piper et al., 2023).

We previously identified serum CCL5 as a negative prognostic marker for late-stage advanced pancreatic cancer(Willenbrock et al., 2021). CCL5 (RANTES) is pro-inflammatory and an acute response to injury or infection that promotes recruitment of monocytes and lymphoid immune cells through CCR5, CCR3, and CCR1. In cancer, sustained CCL5-mediated inflammation leads to a suppressive environment via attraction of $CCR5^{+}$ immunoregulatory components, including Tregs, tumor-associated macrophages (TAMs), and myeloid-derived suppressor cells (MDSCs) normally involved in resolving inflammatory events (Hemmatazad and Berger, 2021). Pancreatic tumors that are poorly differentiated produce higher levels of CCL5 and express more of its main receptor, CCR5, compared to well-differentiated and non-cancerous tissue(Monti et al., 2004; Singh et al., 2018). Disrupting this loop by the FDA-approved CCR5 inhibitor maraviroc reduces pancreatic tumor cell migration, invasiveness(Singh et al., 2018) and proliferation(Huang et al., 2020). Silencing CCL5 expression in Panc02 cells or systemic administration of the CCR5 inhibitor TAK-779 reduces Treg migration and tumor volume in a murine subcutaneous tumor model(Tan et al., 2009). These studies suggest that the CCL5/CCR5 axis may be a promising therapeutic target in pancreatic cancer as it has the potential to alter both the intrinsic properties of tumor cells and immune cell migration.

In established pancreatic tumors, the immune suppressive environment promotes more tissue repair/resolution signaling (M2-like macrophages, MDSCs) and prevents pro-inflammatory signaling (M1-like macrophages). Radiotherapy is delivered to localized tumors to stimulate a pro-inflammatory environment and increase the opportunity for tumor neo-antigens to be recognized by infiltrating adaptive response cells. As such, stereotactic ablative radiotherapy (SBRT) delivers high doses of radiotherapy in a minimal number of fractions to maximize an inflammatory cascade but the sensitivity of lymphocytes to DNA damage and the immune suppressive environment prevent benefit

or meaningful tumor control(Mills et al., 2022). In NSCLC, single cell RNA sequencing (scSeq) of immune cells within tumors identifies a distinct subset of CD49a$^+$ CD103$^+$ tissue-resident memory (TRM) CD8$^+$ T cells that have capacity to respond to neo-antigens but are suppressed(Caushi et al., 2021). In this case, the use of an anti-PD1 antibody (αPD1) supports TRM activation but additional disruption of the immune suppressive environment is still required, indicating that additional components are required in addition to simply activating CD8$^+$ T cell neo-antigen recognition.

Kirchhammer et al. recently reported that a tissue-resident NK (trNK) cell population is induced in NSCLC in response to viral delivery of IL-12, which crucially supported type I conventional dendritic cell (cDC1) infiltration and increased DC-CD8$^+$ T cell interactions(Kirchhammer et al., 2022). Together with PD1 blockade, IL-12-mediated recruitment of trNK cells enhances cross-presentation of antigen to CD8 T via cDC1 suggesting this represents a substantial barrier for T cell focused therapy and that improving the NK/DC/T-cell crosstalk can promote antitumor immunity and tumor control. Notably, this was dependent on CCL5 and points to a positive role for inflammatory CCL5 signaling in the absence of CCR5-mediated suppression(Kirchhammer et al., 2022).

Given the negative prognosis associated with high CCL5 serum levels in human patients and its diverse functions in chemokine and paracrine signaling (Aldinucci et al., 2020), we hypothesized that inhibiting CCR5 rather than CCL5, in combination with radiotherapy and anti-PD1 immunotherapy may improve tumor control via a multimodal approach. To test this, we employed a murine orthotopic pancreatic cancer model and monitored tumor growth and immune infiltration. We find that while the use of a CCR5 inhibitor (CCR5i) alone restricts Treg involvement, it does not impact tumor viability alone or together with αPD1. However, in combination with radiotherapy, we see a significant alteration in MDSCs, NK and CD8 T cells and better tumor control. Interestingly, we observe that IR/CCR5i/αPD1 combination treatment induced a trNK population that is the highly correlated immune population with tumor control. Exploration of scRNA-seq datasets from human PDAC studies confirms the presence of trNK cells as immunomodulatory in human PDAC, and directly supports cDC1-CD8 communication. Strikingly, a specific trNK signature indicates that higher levels of this NK subtype are significantly correlated with better PDAC patient overall and disease-free survival. Moreover, pan-cancer analysis reveals trNK cell involvement is associated with better patient survival across a number of solid tumors and supports the potential utility of a combination regimen comprising ionizing radiation (IR) and CCR5i/αPD1 immunotherapy (IO) as a promising strategy to increase NK/cDC1/CD8 mediated tumor control in solid cancers.

Results

CCL5 is a negative prognostic marker in pancreatic cancer

We previously identified serum CCL5 as a *bona fide* negative prognostic marker for pancreatic cancer(Willenbrock et al., 2021), and found that, in two independent PDAC cohorts (CPTAC3(Cao et al., 2021) and TCGA(Uhlen et al., 2017)), higher CCL5 expression associates with poor overall and disease-free survival, confirming the negative implication of high levels of CCL5 in pancreatic cancer (Figure 1A). To understand the cause of CCL5-mediated reduced survival in PDAC, we hypothesized that immune cells responsive to a CCL5 chemotactic gradient (through expression of the cognate receptors CCR5, CCR3 or CCR1) could be potential contributors to an adverse tumor immune environment (Figure 1B, figure supplement 1A). Single cell sequencing of human tumors has revealed genetic signatures for myeloid derived suppressor cells of polymorphonuclear (PMN-MDSC) or monocytic (M-MDSC) origin(Alshetaiwi et al., 2020), TAMs(Wang et al., 2021), CD4 T-regulatory cells (Treg)(Mijnheer et al., 2021) and NK cells(Smith et al., 2020), but none of these immune populations have yet been implicated as a causative agent in the poor outcome associated with high CCL5 expression in PDAC (Figure 1C). Notably, exploration of individual genes within these signatures indicated stark opposing correlations within each signature pool – particularly for genes associated with MDSCs (S100P vs ARG2) and NK cells (CD56 vs CD16) (Figure 1C, figure supplement 1B). CD56 (*NCAM1*) is a key marker that represents functionally distinct subpopulations of NK cells where $CD56^{bright}$ NK cells represent naïve states that move to $CD56^{dim}$ upon maturation to full cytotoxic potential, whereas conversely $CD16^{+}$ expression marks activation and $CD16^{-}$ immature or quiescent NK cells(Poli et al., 2009). Thus, these distinct subtypes may differentially contribute to survival, e.g., association of CD16 with poor survival may implicate a detrimental role of $CD56^{dim}CD16^{+}$ NK cells, whereas the strong positive prognosis associated with CD56 expression could indicate benefit of $CD56^{bright}CD16^{-}$ NK cells. The benefit of CD56 can be attributed to NK cells over neuronal expression as the neuronal-cell specific homolog *NCAM2* has no prognostic value (figure supplement 1C).

CCR5i modulates Treg infiltration in an orthotopic pancreatic tumor model

We next employed a syngeneic orthotopic pancreatic cancer model where cells derived from $Kras^{G12D}$, $Trp53^{R172H}$, *Pdx1-Cre* C56/BL6 tumor bearing mice are injected into the pancreas of wildtype C56/BL6 mice recapitulating a human pancreatic cancer microenvironment(Matzke-

Ogi et al., 2016). From a selection of independently isolated KPC derived cell lines, we first determined the cell line KPC_F as an appropriate model for human PDAC tumor based on expression of epithelial (E-cadherin), mesenchymal (vimentin), stromal (Collagen I, αSMA) markers as well as displaying both growth kinetics (determined by MRI) amenable for the study and expression of high levels of CCL5 (Figure 2A, figure supplement 2A/B). To address which immune subsets are involved in CCL5 signaling in pancreatic cancer, we developed a 17-color spectral flow cytometry panel to monitor the tumor-infiltrating immune microenvironment in parallel, (figure supplement 2C) and employed a specific CCR5 inhibitor (Maraviroc, CCR5i), to block CCR5, the most widespread and highest-affinity receptor for CCL5 expressed on Tregs (figure supplement 1A).

Pilot experiments injecting 500 KPC-F cells yielded robust and replicative growth kinetics (indicated by matching volumes of ±100 mm^3 at the beginning of exponential growth), permitting direct comparisons of infiltrating immune cells across different treatment groups (Figure 2A). Next, tumors were allowed to reach 50 mm^3 (approx. 12 days) before initiation of treatment with daily CCR5i for 7 days. Mice were culled 30 days post-treatment for the characterization of infiltrating immune cells (Figure 2B). Notably, CCR5i significantly reduced Treg infiltration but had no effect on the infiltration of other immune cells, indicating the active recruitment of $CCR5^+$ Tregs in PDAC (Figure 2B). Given the limited effect of CCR5i on tumor growth kinetics and immune infiltration, however, standalone inhibition of CCR5 and the resultant lack of recruitment of Tregs alone are unlikely to impact PDAC progression.

Combination immunotherapy following localized damage alters tumor of immune composition

Induction of a localized inflammatory microenvironment with ionising radiation (IR) can drive anti-tumor responses, but radiotherapy has had limited success in treatment of PDAC and combination with immune checkpoint inhibitors (e.g. αPD1) does not increase benefit. Therefore, we next examined whether the addition of CCR5i to tumor-targeted IR could overcome this by further modulating immune cell migration, in particular by reducing Treg involvement (Figure 3A, figure supplement 3A). As expected, radiotherapy (3 x 4Gy) produced a strong effect on gross tumor volume, significantly reducing volumes over standalone treatment with αPD1, CCR5i or CCR5i+αPD1 (Figure 3A). Responses to combination of IR with CCR5i, αPD1 or CCR5i+αPD1 (IR+IT) showed larger variations

compared to IR alone, implying mixtures of 'responders' and 'non-responders' to immune-modulatory treatments. Moreover, IR/CCR5i/αPD1 treated tumor sections had significantly reduced DAPI$^+$ and p53$^+$ KPC cells compared to all other conditions, suggesting significantly more loss of tumor cells by triple combination treatment (Figure 3B, figure supplement 3B-C). Tumor sections from the triple combination treatment also presented with increased loss of active stroma (αSMA staining, figure supplement 3D) and increased necrotic areas over standalone radiotherapy (Figure 3C). In line with apparent increased tumor control, the triple combination treatment demonstrated infiltration of CD8$^+$ T cells (Figure 3D), supporting greater penetration of CD8$^+$ T cells into the centre of tumors (figure supplement 3E). These results support improved tumor control with combination of IR+CCR5i+αPD1 over standalone radiotherapy or IR in combination with αPD1 and CCR5i alone. To elucidate the immune mechanisms behind this control, we analysed the immune infiltrate of pancreatic tumors. In line with the results above, the triple combination reduced Treg infiltration, enhanced CD8$^+$ T cell infiltration and supported a moderate increase in CD4$^+$ T helper cells (Figure 3E, figure supplement 3F).

Interestingly, no alteration was seen in the myeloid compartment, except for a reduced infiltration of PMN-MDSCs, whereas a significant infiltration of NK and NKT cells could be observed in pairwise comparisons between IR+αPD1 vs IR+CCR5i or IR+CCR5i+αPD1 (Figure 3E, figure supplement 3F). These results collectively support the notion that IR/CCR5i/αPD1 combination treatment alters immune infiltration by reducing Tregs and increasing NK and CD8 T cells, thereby resulting in greater local tumor control.

CD8 and NKG2D$^-$ NK cells correlate with increased tumor control

To derive more granularity on the potential roles of NK- and T-cell populations in tumor control, tissue sections were stained using an optimized multiplex immunofluorescence panel and analyzed by HALO AI software to identify tumor cells (E-cadherin$^+$ - blue), CD8$^+$ T cells (CD3$^+$CD8$^+$ - orange), CD4$^+$ T-cells (CD3$^+$CD8$^-$ - green) and NK cells (CD3$^-$CD8$^-$NK1.1$^+$ - red) (Figure 4A, figure supplement 4A). As observed with flow cytometric and immunohistochemical analyses, multiplex staining of tumor sections also revealed a significant increase of CD8$^+$ T cells per mm^3 when IR was used in combination with CCR5i or CCR5i/αPD1 (figure supplement 4B). Notably, despite having responders and non-responders in the combination groups (Figure 4A), a significant overall reduction in E-cadherin$^+$ tumor

cells as a percentage of total DAPI^{+} cells was observed (Figure 4B), supporting a decrease in cellularity and an increase in tumor necrosis with the IR/CCR5i/αPD1 combination (Figure 3B,C). The increase in CD8^{+} T cells with combination treatment appears independent of tumor area and is matched by a similar increase in NK cells (Figure 4B, figure supplement 4B). To correlate immune infiltration against loss of tumor cells (a measure of local tumor control) we determined relationships between CD4 T, CD8 T and NK cell populations and E-cadherin^{+} cells across all tumor sections (independent of treatment) and found a significant inverse correlation for both CD8 T and NK cells (r^2=-0.3, p=0.038 and r^2=-0.33, p=0.026 respectively), but not CD4 T cells (Figure 4C).

We next checked if the association between NK cells and loss of tumor cells was due to killing by functionally active NK cells by focusing our analysis on the NKG2D^{+} NK cell population, given that this is one of the major activating receptors on NK cells and is required for the lysis of target cells(Bryceson and Ljunggren, 2008). Surprisingly, the proportion of infiltrating CD3^{-}CD161^{+}NKG2D^{+} cells (NK^{Active}) is reduced under IR/CCR5i/αPD1 combination treatment, implying a decrease in total NK cell cytolytic capacity (figure supplement 4C). The reduced NKG2D expression on NK cells may be a result of the prolonged engagement by ligands expressed on tumor cells, followed by ligand-induced endocytosis and degradation(Quatrini et al., 2015), or the shedding of NKG2D ligands by tumor cells(Kaiser et al., 2007). In both instances, receptor down-regulation causes a reduction in cytotoxicity and impairs NK cell responsiveness to tumor cells, potentially contributing to exhaustion(Groh et al., 2002). Not surprisingly, the reciprocal CD3^{-}CD161^{+}NKG2D^{-} population increases upon triple combination treatment (figure supplement 4C). Interestingly, circulating NK cells from PDAC patients show reduced NKG2D levels compared to healthy controls(Peng et al., 2013) supporting the notion that chronic exposure to NKG2D ligands expressed or shed by PDAC cells might cause NKG2D down-modulation and a hyporesponsive phenotype. Surprisingly, the correlation of NK cells with decreased frequency of E-cadherin^{+} cells was completely abrogated with selection for more functionally competent NK cells (NK^{Active}), implying the opposite hypofunctional NKG2D^{-} NK population (NK$^{NKG2D\text{-}ve}$) is responsible for correlation of NK cells with E-cadherin loss and indeed, a superior inverse correlation is observed for NK$^{NKG2D\text{-}ve}$ and Ecadherin compared to NK^{Active} or NK^{Total} (r^2=-0.52, p=0.003) (Figure 4D). To explore this association is relation to tumor control, sections were split into either E-cadherin^{high} or E-cadherin^{low} and the extent of immune involvement was represented as a

235 percentage of total DAPI^{+}. While CD8 T cells significantly segregated with E-cadherin^{low},
236 implying a contribution to tumor control, the association of NK$^{NKG2D\text{-}ve}$ was vastly more
237 significant (Figure 4E).

238 **Heterogenous subsets of NK cells in PDAC exhibit differential inhibitory and activatory signatures**

239 To extrapolate our findings to the human setting, we explored scRNA-seq data from selected
240 NK and T-cells derived from human pancreatic cancer patients. A total of 51,561 cells were
241 catalogued into 17 distinct cell lineages annotated with canonical gene signatures as
242 described in Steele *et al.* using unsupervised clustering(Steele et al., 2020) (figure supplement
243 5A). UMAP projection of the lymphocyte compartment does not delineate NK subpopulations
244 and shows overlap with CD8 T cells (figure supplement 5B). Therefore, we focused on UMAP
245 projections of the CD8 and NK compartment alone to reveal three clear NK subpopulations
246 that are distinct from CD8 T cells and clearly separate out in clusters of immature (NK_C3),
247 active (NK_C2) and reduced activation (NK_C1) NK cells from T cells (Figure 5A). In agreement
248 with downregulation of circulating NKG2D^{+} in PDAC patients, NKG2D (KLRK1) expression was
249 below detection across all CD8 and NK subpopulations retrieved from patient tumors(Groh et
250 al., 2002). As expected, CD16^{high} (FCGR3a) cytotoxic NK cells (NK_C3) cluster separately from
251 CD16^{-} NK cells (NK_C1) which are more enriched for genes related to cytokine secretion than
252 cytolytic function (Figure 5D, figure supplement 5C). The NK_C1 cluster correlates best with
253 the hypofunction NK phenotype observed in mice as similarly displayed reduced activation
254 (reduced NKG7, NKp80, GZMA and PRF1) with additional expression of tissue residency
255 markers *CD103*, *CD49a* and, surprisingly, the adaptive activating receptor NKG2C (*KLRC2*)
256 (Figure 5B, C). While adaptive-like NK cells in circulating are associated with a Cd56^{dim}CD16^{+}
257 phenotype, adaptive like (i.e. NKG2C^{+}) tissue resident NK cells have been identified in lung
258 tissue(Brownlie et al., 2021) and appear to match our pancreatic tissue NK_C1 cells.
259 Downstream UMAP analysis of the NK cell population distinguishes these 3 subsets of NK
260 cells (NK_C1, NK_C2 and NK_C3) based on 41 differentially expressed genes (Figure 5D, E).
261 Given that CD56 expression correlates with increased survival in PDAC patients
262 (Figure 1C) we were intrigued to notice that the hypofunctional NK_C1 cluster is enriched for
263 CD56 but not CD16 expression (Figure 5D). These data suggest that NK_C1 cluster represents
264 a subset of NK cells in PDAC that display tissue-residency markers (*ITGAE,* CD103 and *ITGA1,*
265 CD49a) and have an immune-secretory phenotype (XCL1) as opposed to cytolytic phenotype

(NK_C2 $CD16^+$, $NKG7^+$) (Figure 5E). Furthermore, we define a core signature gene set to distinguish NK_C1 from other NK subpopulations (Figure 5F). Verification of the NK_C1 population as $NKG2C^+$ and tissue resident (trNK) in a second scRNA pancreatic cancer dataset of Peng *et al.*(Peng et al., 2013) confirmed the existence of these cells in an independent PDAC cohort, again hypofunctional for cytotoxic activity and enriched for the inhibitory receptor NKG2A (KLRC1) (figure supplement 5D, E, F).

Tissue resident NK cells in PDAC show differential communication

The NK_C1 population had the highest expression of the chemokines XCL1 and XCL2, which have been demonstrated to attract type-1 conventional dendritic cells (cDC1)(Böttcher et al., 2018) and thereby increase cross presentation to $CD8^+$ T cells. We next explored myeloid populations in the Steele *et al.* scPDAC dataset (figure supplement 6A) and identified cDC1 cells as $XCR1^+$ enriched compared to other DC subsets (Figure 6A, figure supplement 6B). As XCR1 is the receptor for XCL1/2, this suggests that a main direction of communication is from NK_C1 cells in PDAC is to cDC1 (Figure 6B). We next employed the R-package 'CellChat'(Jin et al., 2021) to further dissect the crosstalk between NK_C1 and other cells found in the pancreatic tumor microenvironment, and confirmed NK_C1-derived XCL1/2 is the strongest signal to $XCR1^+$ cDC1s (Figure 6C). Analysis of specific ligand-receptor pairs between NK_C1 and 24 other cell groups yielded 32 significant interactions, of which the TNFSF14 (LIGHT)-TNFRSF14 pair was the most universal intercellular interaction, whereas CD74 (or MIF) signaling showed the highest communication probability (figure supplement 6C).

Within the immune cell compartment, communication signals between NK_C1 and macrophages were the most abundant and diverse, followed by cDCs (cDC2 and cDC1) and Tregs (figure supplement 6C). Similarly, cDC1 from in these PDAC samples capable of presenting MHC class I peptides to $CD8^+$ T cells, but surprisingly also MHC class II to $CD4^+$ Tregs (figure supplement 6D). Next, significant receptor-ligand interactions were segregated as 'outgoing' or 'incoming' signals to understand directionality of communication. Among the outgoing signals from different cell types, NK_C1 cells contributed the highest IL-16, CSF, LIGHT (TNFSF14), FASLG and MIF signals in tumors (Figure 6D). IL-16 is mainly known as a chemoattractant for $CD4^+$ T cells, however $CD4^+$ dendritic cells exist and have also been demonstrated to be recruited by IL-16 (Bialecki et al., 2011; Kaser et al., 1999; Vremec et al., 2000). IL-16 has also been described to increase HLA-DR levels in $CD4^+$ T cells and

297 eosinophils, therefore has the potential to induce MHC antigen presentation in $CD4^+$
298 cells(Cruikshank et al., 1987; Rand et al., 1991). Taken together, these interactions support
299 the hypothesis that trNK cells may improve tumor control via recruitment of type 1 dendritic
300 cells via XCR1, while promoting DC maturation via LIGHT-CD86(Zou and Hu, 2005) signaling
301 and supporting antigen presentation to both $CD4^+$ and $CD8^+$ T cells via MIF-CD74 signaling
302 (Basha et al., 2012) (Figure 6E). On the other hand, dendritic cell-secreted BAG6 may
303 promote both survival and cytokine release by NK cells by binding NKp30(Simhadri et al.,
304 2008) and directly signal to CD8 T cells via CXCL16-CXCR6(Di Pilato et al., 2021), thereby
305 generating an anti-tumor feedforward loop (Figure 6E). Remarkably, IL-16 also communicates
306 to $CD4^+$ Tregs and $CD74^+$ fibroblasts, likely supporting tumor growth (Figure 6D). However,
307 both cell types may be susceptible to Fas-mediated cell death due to NK_C1 expression of Fas
308 ligand (Figure 6D). This could enhance immune cell infiltration and revoke the
309 immunosuppressive environment, ultimately contributing to increased tumor control.

310 These results so far suggest the presence of immunoregulatory trNK cells in PDAC that
311 are involved in an intricate immune communication network with DCs and CD8 T cells to
312 enhance anti-tumor immunity. To support this hypothesis, we explored the correlation
313 between trNK and CD8 T infiltration in our KPC_F orthotopic tumor model and found a highly
314 significant positive association (R^2 = 0.6571, p = 0.003) which was strengthened when we
315 focused on untreated (Mock) versus IR+IT combinations where trNK cells are evident (R^2 =
316 0.9223, p = 0.0004) (Figure 6F). To ascertain if this also holds true in human PDAC, we first
317 specified the NK_C1 signature as a 14-gene signature that was specific for our tissue-resident
318 NK cells over all other cells to distinguish levels in bulk datasets (Table 1). We next explored
319 the CD8 T:trNK cell relationship in PAAD_TCGA and, as the model in Figure 6E predicts this
320 interaction to be cDC1 dependent, by binning PAAD_TCGA cohort into quartiles based
321 differential cDC1 signature expression to test dependence of CD8 T:trNK on cDC1 levels
322 (Figure 6G). PDAC patient tumors with the lowest evidence for cDC1 involvement have a
323 weak correlation of trNK_C1 with CD8A and CD8B (p = 0.047; p = 0.45 respectively) which
324 rises to a strong highly significant correlation when the highest levels of cDC1s are present
325 (R^2 0.3, trNK_C1 vs CD8A p = 0.0001; R^2 0.34, trNK_C1 vs CD8B p = 0.000047) (Figure 6G).

326 **NK cell signature correlates with improved survival**

As the presence of trNK and correlation with CD8 T cells appears boosted by IR, we next explored our original finding that CD56 correlates with highly significant survival in PDAC (Figure 1, figure supplement 1). We hypothesized that tumors with a high *CD56* signature might recruit a high proportion of trNK ($CD56^{bright}CD16^{low}$), whereas tumors with a low CD56 signature might have a lower proportion of trNK and, therefore, could benefit from IR. Indeed, separating PAAD_TCGA patients into those who received radiotherapy (RTx) versus those that did not, showed that the benefit in overall survival of PDAC patients is only apparent in the $CD56^{low}$ patient group (log rank p <0.0001, Figure 7A). We next explored whether CD56-associated survival is specifically due to the presence of trNK cells using our NK_C1 signature (Table 1). Analysis of primary PDAC tumors from the TCGA (TCGA_PAAD) demonstrates that patients with tumors enriched for the trNK cell (NK_C1) gene signature were associated with improved PDAC survival compared to patients without trNK involvement (Figure 7B, figure supplement 7A). Similarly to $CD56^{low}$ patients, we find that patients with $trNK^{low}$ benefit from RTx (log rank p <0.005, Figure 7C). Notably, we find that despite an overall poor prognosis, $CCL5^{high}$ patients (TCGA and CPTAC3) are significantly enriched for the trNK_C1 gene signature (Figure 7D), potentially due to strong CCR5 or CCR1-mediated recruitment (figure supplement 1A). However, as CCL5 also recruits MDSCs, TAMs, Tregs and conventional NK cells via CCR5, CCR5i prevents a tumor suppressive microenvironment, both directly and indirectly by retaining trNK cells that remove Tregs through FASL (figure supplement 7B). Therefore, we could expect that patients with $CCL5^{high}$ NK_C1^{low} would perform significantly worse than patients with $CCL5^{high}NK\_C1^{high}$. Indeed, $CCL5^{high}$ patients enriched for the NK_C1 signature or CD56 had significantly improved overall and disease-free survival (Figure 7E, F). This also supports a model where CCL5 mediated recruitment of NK cells can be beneficial in the absence of CCL5-CCR5 recruitment, via CCR1(Ajuebor et al., 2007) (figure supplement 7C, 1A). These results suggest that despite high CCL5 levels and an overall poor prognostic outcome, the presence of tissue-resident NK cells significantly improves survival and provides an opportunity for intervention with the IR+IT combination.

Finally, we explored whether the NK_C1 gene signature could be a prognostic marker in solid malignancies other than PDAC by expanding our TCGA analysis. The majority of cancers with enriched expression of our NK_C1 gene signature showed improved survival apart from endometrium and prostate (Figure 8), as a continuous variable or as a high vs low

359 in a univariate Cox regression (figure supplement 8A,B). The latter result confirms our
360 hypothesis that enrichment of trNK cells is a protective factor across most solid malignancies.
361 Moreover, the ability to enrich for this population with IR/IO combinatorial strategies
362 supports the idea that trNK cells generally improve overall survival though improving CD8 T
363 cell activity in solid cancers.
364

Discussion

Novel approaches such as immunotherapies struggle to improve outcome in PDAC as tumors are stromal rich, myeloid-involved immunosuppressive microenvironments devoid of cytotoxic lymphocytes. Most strategies to combat immune suppression, e.g. targeting inhibitory checkpoints such as PD1/PDL1, fail as single therapies because PDAC is largely devoid of the CD8 T cells these agents are designed to reactivate. Combining them with inhibitors of myeloid suppression (e.g. CXCR2) to increase CD8 T penetration also failed to impact survival in clinical trials despite showing promise in pre-clinical studies(Steele et al., 2015),(Siolas et al., 2020). Similarly, high-dose hypo-fractionated ablative radiotherapy has been employed to create an acute localized inflammatory response to stimulate intra-tumoral penetration of CD8 T cells, but even in conjunction with PD1/PDL1 blockade this approach has not shown benefit in PDAC(Parikh et al., 2021). Novel strategies in pre-clinical PDAC models comprising ionizing radiation (IR), αPD1 and BMS-687681 (a dual CCR2/CCR5 inhibitor) have shown promising increases in CD8 T cells(Wang et al., 2022) whereas the combination of IR and the bifunctional agent αPD-1/IL-2Rβγ stimulates tumor penetration of polyfunctional stem-like activated CD8 T cells and $DNAM1^{+}$ cytotoxic natural killer (NK) cells(Piper et al., 2023). Together, these approaches indicate potential benefits of a coordinated alteration of the suppressive microenvironment and checkpoint blockade to reduce regulatory T cells (Tregs) and increase NK cell infiltration in addition to supporting CD8 T cell activity. The utility of RT for localized PDAC has been controversial but innovative technology can now deliver ionizing radiation at higher-doses with greater precision(Mills et al., 2022). Rather than simple ablative radiotherapy, this strategy is being employ to increase localized damage that stimulates an acute damage response in immune-cold tumors or increase tumor neoantigens to stimulate adaptive responses(Sodergren et al., 2020). In support of this, the use of IR alongside αPD-1/IL-2Rβγ or FAKi appeared to induce durable immunity in preclinical models(Lander et al., 2022; Piper et al., 2023), suggesting the induction of immunologic memory against tumor antigens is possible.

We were led by our previous clinical trial results implicating serum CCL5 levels as a negative prognostic marker for PDAC survival, which we now validate in two independent validation datasets. CCL5 has both pro-inflammatory roles as a chemoattractant for leukocytes and anti-inflammatory activity via recruitment of $CCR5^{+}$ Tregs(Tan et al., 2009). To maintain beneficial

signals but limit pro-tumorigenic signaling, we targeted CCR5 alone using maraviroc. Not surprisingly, in an orthotopic KPC model of PDAC we found that Tregs were restricted by CCR5i directly, and the combination of IR and immunotherapy+(IT, CCR5i, αPD1 or CCR5i/αPD1) correlates with a progressive enrichment of CD8 T cells. Intriguingly, CD8 T cells alone were insufficient to explain the loss of cellularity or the increase in necrotic tumors seen with the IR/CCR5i/αPD1 combination, but we do observe a significant increase in total NK and NKT cells that correlates with better local control.

NK infiltration has been associated with positive outcomes in many solid tumors, considered to be due to the positive impact of cytotoxic NK cells in cytotoxic CD8 T-mediated tumor clearance(Nersesian et al., 2021). However, the data supporting the independent contribution of NK activity is difficult to discern due to overlap of expression profiles of cytotoxic cells. Surprisingly, markers of cytotoxic cells or specific CD8/CD4 lymphocyte receptors do not perform as indicators of survival from bulk mRNA datasets (Figure 5). This may be due to sensitivity issues but, more likely, the presence of cytotoxic cells alone does not necessarily indicate beneficial responses in patients(Nersesian et al., 2021). This is supported by the limited efficacy of immunotherapy strategies to tumors with a high mutational burden. NK cells represent a variety of subsets defined by surface markers, found in the periphery (circulating), secondary lymphoid organs (spleen, lymph nodes), and specific tissues (e.g. lung, liver, uterus) where markers of tissue residency increase retention or prevent egress(Hashemi and Malarkannan, 2020). In addition to tissue-resident NK cells, tumors appear to accumulate NK populations that become less cytotoxic through downregulation of activating receptors, (NKG2D, NKp40, NKp44) and increased expression of inhibitory receptors (NKG2A) or repression/exhaustion markers (e.g. TIGIT, TIM3) (Hashemi and Malarkannan, 2020) (Marcon et al., 2020). Importantly, NK tissue-resident or hypoactivated subsets commonly display a reduction in cytotoxicity but become highly active immunomodulatory players via expression of XCL1 and XCL2(de Andrade et al., 2019). In melanoma, NK-mediated expression of XCL1 is crucial for the migration of $XCR1^{+}$ conventional type 1 dendritic cells (cDC1) and therefore the non-cytotoxic NK subsets in tumors may be vital for cDC1-mediated cross-presentation of tumor antigens to CD 8 T cells(Böttcher et al., 2018). This may explain why levels of CD8 T cells in tumors or removal of inhibitory signaling is insufficient to gain tumor control. Thus, therapeutic strategies aimed at

increasing the presence of cDC1 or NK cells may work in combination to support treatments that induce CD8 T cell activity.

Our data suggest that combination therapy to stimulate an acute inflammatory response (IR) together with CCR5i/αPD1 (IT) sufficiently modulates the tumor immune microenvironment to improve tumor control. As frequently observed in solid tumors, reduction of cancer cells correlates with intra-tumoral infiltration of NK cells ($CD56^{bright}CD16^{-}$) and improved CD8 T cell penetration(Wu et al., 2020). Surprisingly, our tumors were penetrated by $NKG2D^{-}$ NK cells, suggesting a population with reduced cytotoxicity (figure supplement 5C) which we correlated to a similar population (NK_C1) identified from scRNAseq of human PDAC samples. This population was $CD56^{+}CD16^{-}NKG2C^{+}$, in keeping with adaptive-like tissue resident NK cells(Brownlie et al., 2021; Ruckert et al., 2022) and the apparent beneficial association of CD56 expression with PDAC survival we identified above. NKG2C is a marker of adaptive-like NK cells during viral infections where they offer a potential memory capability to innate immunity(Brownlie et al., 2021; Lopez-Botet et al., 2023). First identified as a subpopulation of blood derived $CD16^{+}$ NK cells in response to viral infection but more recently found to be independent of CD16 expression in tissue (Brownlie et al., 2021). Notably, these were marked with receptors for tissue residency CD103 (*ITGAE*), CD49a (*ITGA1*), chemokine expression (XCL1/2) and lymphocyte exhaustion markers TIM3 (*HAVCR2*), TIGIT, *TNFRSF4*), potentially suggesting conversion of cytotoxic NK cells to an adaptive-like immunomodulatory phenotype that can persist in tissues (Brownlie et al., 2021; Ruckert et al., 2022). Single cell RNAseq from PDAC tissue confirm that trNKs are likely to mediate recruitment of cDC1s via XCL1-XCR1, but communicate additional signals, including IL-16, LIGHT (*TNFSF14*) and MIF-CD74 which have the potential to upregulate MHC-I expression, presentation and co-stimulatory molecules to contribute to cross presentation(Basha et al., 2012; Cruikshank et al., 1987; Zou and Hu, 2005). We also find that trNK may also recruit $CD4^{+}$ Tregs via IL16 but concomitant FAS-signaling would lead to Treg apoptosis and support tumor control (Figure 5E, 6D).

Strikingly, using our signature we find that elevated involvement of trNKs in PDAC correlates with CD8 T cell recruitment in a cDC1-dependent manner. Moreover, this supports a model where the inactivation of cytotoxic NK cells in tumors appears to be a conversion to immunomodulatory trNKs and an important mechanistic switch from innate to adaptive immunity. Our therapeutic strategy of short ablative radiation-induced damage (IR) followed

459 by CCR5i/αPD1 (IT) offers a potential regimen to increase disease free survival in PDAC.
460 Finally, trNK-like cells with similar traits are increasingly being observed across a variety of
461 cancers(Brownlie et al., 2023; Kirchhammer et al., 2022; Marquardt et al., 2015). Finally, our
462 signature identifies patients with a significant survival benefit across 14 tumor types,
463 indicating a universal phenomenon attributable to this hypo-cytotoxic immunomodulatory
464 NK subset.

Author contributions

Conceptualization, S.M., EO'N. Methodology, S.L., S.H., C.D. Investigation; S.L., S.H., S.G., C.D. E.AJ. Formal analysis, S.G., S.H., C.D., E.AJ. Data curation, S.G., S.L., S.H., C.D., H.F., S.S. Funding acquisition: M.R.M., J.M, E.O'N. Project administration: E.O'N. Supervision: K.J., E.O'N. Writing – original draft, S.G, C.D, E.O'N. Writing – review & editing, S.G., R.BR., G.V., J.M., K.J., E.O'N. All authors read and approved the manuscript.

Acknowledgements

Authors thank the oncology preclinical imaging core (S.Smart, V.Kersemans, PD.Allen, M. Hill and JM Thompson) for providing contracted small animal MRI and radiotherapy services, Biomedical Services (K.Watson) and H. Xu for technical support. Funding: Kidani Memorial Trust, Cancer Research UK, Precision Panc (A25233), CRUK Beatson Institute (A31287, A29996) and CRUK Scotland Centre (CTRQQR-2021\100006). Medical Research Council.

References

Ajuebor, M. N., Wondimu, Z., Hogaboam, C. M., Le, T., Proudfoot, A. E., and Swain, M. G. (2007). CCR5 deficiency drives enhanced natural killer cell trafficking to and activation within the liver in murine T cell-mediated hepatitis. Am J Pathol *170*, 1975-1988.

Aldinucci, D., Borghese, C., and Casagrande, N. (2020). The CCL5/CCR5 Axis in Cancer Progression. Cancers (Basel) *12*.

Alshetaiwi, H., Pervolarakis, N., McIntyre, L. L., Ma, D., Nguyen, Q., Rath, J. A., Nee, K., Hernandez, G., Evans, K., Torosian, L.*, et al.* (2020). Defining the emergence of myeloid-derived suppressor cells in breast cancer using single-cell transcriptomics. Sci Immunol *5*.

Basha, G., Omilusik, K., Chavez-Steenbock, A., Reinicke, A. T., Lack, N., Choi, K. B., and Jefferies, W. A. (2012). A CD74-dependent MHC class I endolysosomal cross-presentation pathway. Nat Immunol *13*, 237-245.

Bialecki, E., Macho Fernandez, E., Ivanov, S., Paget, C., Fontaine, J., Rodriguez, F., Lebeau, L., Ehret, C., Frisch, B., Trottein, F., and Faveeuw, C. (2011). Spleen-resident CD4+ and CD4- CD8alpha-dendritic cell subsets differ in their ability to prime invariant natural killer T lymphocytes. PLoS One *6*, e26919.

Bockorny, B., Semenisty, V., Macarulla, T., Borazanci, E., Wolpin, B. M., Stemmer, S. M., Golan, T., Geva, R., Borad, M. J., Pedersen, K. S.*, et al.* (2020). BL-8040, a CXCR4 antagonist, in combination with pembrolizumab and chemotherapy for pancreatic cancer: the COMBAT trial. Nat Med *26*, 878-885.

Böttcher, J. P., Bonavita, E., Chakravarty, P., Blees, H., Cabeza-Cabrerizo, M., Sammicheli, S., Rogers, N. C., Sahai, E., Zelenay, S., and Reis e Sousa, C. (2018). NK Cells Stimulate Recruitment of cDC1 into the Tumor Microenvironment Promoting Cancer Immune Control. Cell *172*, 1022-1037.e1014.

Brownlie, D., Scharenberg, M., Mold, J. E., Hard, J., Kekalainen, E., Buggert, M., Nguyen, S., Wilson, J. N., Al-Ameri, M., Ljunggren, H. G.*, et al.* (2021). Expansions of adaptive-like NK cells with a tissue-resident phenotype in human lung and blood. Proc Natl Acad Sci U S A *118*.

Brownlie, D., von Kries, A., Valenzano, G., Wild, N., Yilmaz, E., Safholm, J., Al-Ameri, M., Alici, E., Ljunggren, H. G., Schliemann, I*., et al.* (2023). Accumulation of tissue-resident natural killer cells, innate lymphoid cells, and CD8(+) T cells towards the center of human lung tumors. Oncoimmunology *12*, 2233402.

Bryceson, Y. T., and Ljunggren, H. G. (2008). Tumor cell recognition by the NK cell activating receptor NKG2D. Eur J Immunol *38*, 2957-2961.

Cao, L., Huang, C., Cui Zhou, D., Hu, Y., Lih, T. M., Savage, S. R., Krug, K., Clark, D. J., Schnaubelt, M., Chen, L*., et al.* (2021). Proteogenomic characterization of pancreatic ductal adenocarcinoma. Cell *184*, 5031-5052 e5026.

Caushi, J. X., Zhang, J., Ji, Z., Vaghasia, A., Zhang, B., Hsiue, E. H., Mog, B. J., Hou, W., Justesen, S., Blosser, R*., et al.* (2021). Transcriptional programs of neoantigen-specific TIL in anti-PD-1-treated lung cancers. Nature *596*, 126-132.

Cruikshank, W. W., Berman, J. S., Theodore, A. C., Bernardo, J., and Center, D. M. (1987). Lymphokine activation of T4+ T lymphocytes and monocytes. J Immunol *138*, 3817-3823.

de Andrade, L. F., Lu, Y., Luoma, A., Ito, Y., Pan, D., Pyrdol, J. W., Yoon, C. H., Yuan, G. C., and Wucherpfennig, K. W. (2019). Discovery of specialized NK cell populations infiltrating human melanoma metastases. JCI Insight *4*.

Di Pilato, M., Kfuri-Rubens, R., Pruessmann, J. N., Ozga, A. J., Messemaker, M., Cadilha, B. L., Sivakumar, R., Cianciaruso, C., Warner, R. D., Marangoni, F*., et al.* (2021). CXCR6 positions cytotoxic T cells to receive critical survival signals in the tumor microenvironment. Cell *184*, 4512-4530 e4522.

Doi, T., Muro, K., Ishii, H., Kato, T., Tsushima, T., Takenoyama, M., Oizumi, S., Gemmoto, K., Suna, H., Enokitani, K*., et al.* (2019). A Phase I Study of the Anti-CC Chemokine Receptor 4 Antibody, Mogamulizumab, in Combination with Nivolumab in Patients with Advanced or Metastatic Solid Tumors. Clin Cancer Res *25*, 6614-6622.

Groh, V., Wu, J., Yee, C., and Spies, T. (2002). Tumour-derived soluble MIC ligands impair expression of NKG2D and T-cell activation. Nature *419*, 734-738.

Hashemi, E., and Malarkannan, S. (2020). Tissue-Resident NK Cells: Development, Maturation, and Clinical Relevance. Cancers (Basel) *12*.

Hemmatazad, H., and Berger, M. D. (2021). CCR5 is a potential therapeutic target for cancer. Expert Opin Ther Targets *25*, 311-327.

Huang, H., Zepp, M., Georges, R. B., Jarahian, M., Kazemi, M., Eyol, E., and Berger, M. R. (2020). The CCR5 antagonist maraviroc causes remission of pancreatic cancer liver metastasis in nude rats based on cell cycle inhibition and apoptosis induction. Cancer Lett *474*, 82-93.

Jin, S., Guerrero-Juarez, C. F., Zhang, L., Chang, I., Ramos, R., Kuan, C. H., Myung, P., Plikus, M. V., and Nie, Q. (2021). Inference and analysis of cell-cell communication using CellChat. Nat Commun *12*, 1088.

Kaiser, B. K., Yim, D., Chow, I. T., Gonzalez, S., Dai, Z., Mann, H. H., Strong, R. K., Groh, V., and Spies, T. (2007). Disulphide-isomerase-enabled shedding of tumour-associated NKG2D ligands. Nature *447*, 482-486.

Kaser, A., Dunzendorfer, S., Offner, F. A., Ryan, T., Schwabegger, A., Cruikshank, W. W., Wiedermann, C. J., and Tilg, H. (1999). A role for IL-16 in the cross-talk between dendritic cells and T cells. J Immunol *163*, 3232-3238.

Kirchhammer, N., Trefny, M. P., Natoli, M., Brucher, D., Smith, S. N., Werner, F., Koch, V., Schreiner, D., Bartoszek, E., Buchi, M*., et al.* (2022). NK cells with tissue-resident traits shape response to immunotherapy by inducing adaptive antitumor immunity. Sci Transl Med *14*, eabm9043.

Lander, V. E., Belle, J. I., Kingston, N. L., Herndon, J. M., Hogg, G. D., Liu, X., Kang, L. I., Knolhoff, B. L., Bogner, S. J., Baer, J. M*., et al.* (2022). Stromal Reprogramming by FAK Inhibition Overcomes Radiation Resistance to Allow for Immune Priming and Response to Checkpoint Blockade. Cancer Discov *12*, 2774-2799.

Lopez-Botet, M., De Maria, A., Muntasell, A., Della Chiesa, M., and Vilches, C. (2023). Adaptive NK cell response to human cytomegalovirus: Facts and open issues. Semin Immunol *65*, 101706.

Marcon, F., Zuo, J., Pearce, H., Nicol, S., Margielewska-Davies, S., Farhat, M., Mahon, B., Middleton, G., Brown, R., Roberts, K. J., and Moss, P. (2020). NK cells in pancreatic cancer demonstrate impaired cytotoxicity and a regulatory IL-10 phenotype. Oncoimmunology *9*, 1845424.

Marquardt, N., Beziat, V., Nystrom, S., Hengst, J., Ivarsson, M. A., Kekalainen, E., Johansson, H., Mjosberg, J., Westgren, M., Lankisch, T. O.*, et al.* (2015). Cutting edge: identification and characterization of human intrahepatic CD49a+ NK cells. J Immunol *194*, 2467-2471.

Matzke-Ogi, A., Jannasch, K., Shatirishvili, M., Fuchs, B., Chiblak, S., Morton, J., Tawk, B., Lindner, T., Sansom, O., Alves, F.*, et al.* (2016). Inhibition of Tumor Growth and Metastasis in Pancreatic Cancer Models by Interference With CD44v6 Signaling. Gastroenterology *150*, 513-525 e510.

Mijnheer, G., Lutter, L., Mokry, M., van der Wal, M., Scholman, R., Fleskens, V., Pandit, A., Tao, W., Wekking, M., Vervoort, S.*, et al.* (2021). Conserved human effector Treg cell transcriptomic and epigenetic signature in arthritic joint inflammation. Nat Commun *12*, 2710.

Mills, B. N., Qiu, H., Drage, M. G., Chen, C., Mathew, J. S., Garrett-Larsen, J., Ye, J., Uccello, T. P., Murphy, J. D., Belt, B. A.*, et al.* (2022). Modulation of the Human Pancreatic Ductal Adenocarcinoma Immune Microenvironment by Stereotactic Body Radiotherapy. Clin Cancer Res *28*, 150-162.

Mohindra, N. A., Kircher, S. M., Nimeiri, H. S., Benson, A. B., Rademaker, A., Alonso, E., Blatner, N., Khazaie, K., and Mulcahy, M. F. (2015). Results of the phase Ib study of ipilimumab and gemcitabine for advanced pancreas cancer. Journal of Clinical Oncology *33*, e15281-e15281.

Monti, P., Marchesi, F., Reni, M., Mercalli, A., Sordi, V., Zerbi, A., Balzano, G., Di Carlo, V., Allavena, P., and Piemonti, L. (2004). A comprehensive in vitro characterization of pancreatic ductal carcinoma cell line biological behavior and its correlation with the structural and genetic profile. Virchows Arch *445*, 236-247.

Nersesian, S., Schwartz, S. L., Grantham, S. R., MacLean, L. K., Lee, S. N., Pugh-Toole, M., and Boudreau, J. E. (2021). NK cell infiltration is associated with improved overall survival in solid cancers: A systematic review and meta-analysis. Transl Oncol *14*, 100930.

Parikh, A. R., Szabolcs, A., Allen, J. N., Clark, J. W., Wo, J. Y., Raabe, M., Thel, H., Hoyos, D., Mehta, A., Arshad, S.*, et al.* (2021). Radiation therapy enhances immunotherapy response in microsatellite stable colorectal and pancreatic adenocarcinoma in a phase II trial. Nat Cancer *2*, 1124-1135.

Peng, Y. P., Zhu, Y., Zhang, J. J., Xu, Z. K., Qian, Z. Y., Dai, C. C., Jiang, K. R., Wu, J. L., Gao, W. T., Li, Q.*, et al.* (2013). Comprehensive analysis of the percentage of surface receptors and cytotoxic granules positive natural killer cells in patients with pancreatic cancer, gastric cancer, and colorectal cancer. J Transl Med *11*, 262.

Piper, M., Hoen, M., Darragh, L. B., Knitz, M. W., Nguyen, D., Gadwa, J., Durini, G., Karakoc, I., Grier, A., Neupert, B.*, et al.* (2023). Simultaneous targeting of PD-1 and IL-2Rbetagamma with radiation therapy inhibits pancreatic cancer growth and metastasis. Cancer Cell *41*, 950-969 e956.

Poli, A., Michel, T., Theresine, M., Andres, E., Hentges, F., and Zimmer, J. (2009). CD56bright natural killer (NK) cells: an important NK cell subset. Immunology *126*, 458-465.

Quatrini, L., Molfetta, R., Zitti, B., Peruzzi, G., Fionda, C., Capuano, C., Galandrini, R., Cippitelli, M., Santoni, A., and Paolini, R. (2015). Ubiquitin-dependent endocytosis of NKG2D-DAP10 receptor complexes activates signaling and functions in human NK cells. Sci Signal *8*, ra108.

Rand, T. H., Cruikshank, W. W., Center, D. M., and Weller, P. F. (1991). CD4-mediated stimulation of human eosinophils: lymphocyte chemoattractant factor and other CD4-binding ligands elicit eosinophil migration. J Exp Med *173*, 1521-1528.

Royal, R. E., Levy, C., Turner, K., Mathur, A., Hughes, M., Kammula, U. S., Sherry, R. M., Topalian, S. L., Yang, J. C., Lowy, I., and Rosenberg, S. A. (2010). Phase 2 trial of single agent Ipilimumab (anti-CTLA-4) for locally advanced or metastatic pancreatic adenocarcinoma. J Immunother *33*, 828-833.

Ruckert, T., Lareau, C. A., Mashreghi, M. F., Ludwig, L. S., and Romagnani, C. (2022). Clonal expansion and epigenetic inheritance of long-lasting NK cell memory. Nat Immunol *23*, 1551-1563.

Simhadri, V. R., Reiners, K. S., Hansen, H. P., Topolar, D., Simhadri, V. L., Nohroudi, K., Kufer, T. A., Engert, A., and Pogge von Strandmann, E. (2008). Dendritic cells release HLA-B-associated transcript-3 positive exosomes to regulate natural killer function. PLoS One *3*, e3377.

Singh, S. K., Mishra, M. K., Eltoum, I. A., Bae, S., Lillard, J. W., Jr., and Singh, R. (2018). CCR5/CCL5 axis interaction promotes migratory and invasiveness of pancreatic cancer cells. Sci Rep *8*, 1323.

Siolas, D., Morrissey, C., and Oberstein, P. E. (2020). The Achilles' Heel of Pancreatic Cancer: Targeting pancreatic cancer's unique immunologic characteristics and metabolic dependencies in clinical trials. J Pancreatol *3*, 121-131.

Smith, S. L., Kennedy, P. R., Stacey, K. B., Worboys, J. D., Yarwood, A., Seo, S., Solloa, E. H., Mistretta, B., Chatterjee, S. S., Gunaratne, P.*, et al.* (2020). Diversity of peripheral blood human NK cells identified by single-cell RNA sequencing. Blood Adv *4*, 1388-1406.

Sodergren, M. H., Mangal, N., Wasan, H., Sadanandam, A., Balachandran, V. P., Jiao, L. R., and Habib, N. (2020). Immunological combination treatment holds the key to improving survival in pancreatic cancer. J Cancer Res Clin Oncol *146*, 2897-2911.

Steele, C. W., Karim, S. A., Foth, M., Rishi, L., Leach, J. D., Porter, R. J., Nixon, C., Jeffry Evans, T. R., Carter, C. R., Nibbs, R. J.*, et al.* (2015). CXCR2 inhibition suppresses acute and chronic pancreatic inflammation. J Pathol *237*, 85-97.

Steele, N. G., Carpenter, E. S., Kemp, S. B., Sirihorachai, V. R., The, S., Delrosario, L., Lazarus, J., Amir, E. D., Gunchick, V., Espinoza, C.*, et al.* (2020). Multimodal Mapping of the Tumor and Peripheral Blood Immune Landscape in Human Pancreatic Cancer. Nat Cancer *1*, 1097-1112.

Tan, M. C., Goedegebuure, P. S., Belt, B. A., Flaherty, B., Sankpal, N., Gillanders, W. E., Eberlein, T. J., Hsieh, C. S., and Linehan, D. C. (2009). Disruption of CCR5-dependent homing of regulatory T cells inhibits tumor growth in a murine model of pancreatic cancer. J Immunol *182*, 1746-1755.

Uhlen, M., Zhang, C., Lee, S., Sjostedt, E., Fagerberg, L., Bidkhori, G., Benfeitas, R., Arif, M., Liu, Z., Edfors, F.*, et al.* (2017). A pathology atlas of the human cancer transcriptome. Science *357*.

Vremec, D., Pooley, J., Hochrein, H., Wu, L., and Shortman, K. (2000). CD4 and CD8 expression by dendritic cell subtypes in mouse thymus and spleen. J Immunol *164*, 2978-2986.

Wang, J., Saung, M. T., Li, K., Fu, J., Fujiwara, K., Niu, N., Muth, S., Wang, J., Xu, Y., Rozich, N.*, et al.* (2022). CCR2/CCR5 inhibitor permits the radiation-induced effector T cell infiltration in pancreatic adenocarcinoma. J Exp Med *219*.

Wang, L., He, T., Liu, J., Tai, J., Wang, B., Chen, Z., and Quan, Z. (2021). Pan-cancer analysis reveals tumor-associated macrophage communication in the tumor microenvironment. Exp Hematol Oncol *10*, 31.

Weiss, G. J., Blaydorn, L., Beck, J., Bornemann-Kolatzki, K., Urnovitz, H., Schutz, E., and Khemka, V. (2018). Phase Ib/II study of gemcitabine, nab-paclitaxel, and pembrolizumab in metastatic pancreatic adenocarcinoma. Invest New Drugs *36*, 96-102.

Weiss, G. J., Waypa, J., Blaydorn, L., Coats, J., McGahey, K., Sangal, A., Niu, J., Lynch, C. A., Farley, J. H., and Khemka, V. (2017). A phase Ib study of pembrolizumab plus chemotherapy in patients with advanced cancer (PembroPlus). Br J Cancer *117*, 33-40.

Willenbrock, F., Cox, C. M., Parkes, E. E., Wilhelm-Benartzi, C. S., Abraham, A. G., Owens, R., Sabbagh, A., Jones, C. M., Hughes, D. L. I., Maughan, T.*, et al.* (2021). Circulating biomarkers and outcomes from a randomised phase 2 trial of gemcitabine versus capecitabine-based chemoradiotherapy for pancreatic cancer. Br J Cancer *124*, 581-586.

Wu, S. Y., Fu, T., Jiang, Y. Z., and Shao, Z. M. (2020). Natural killer cells in cancer biology and therapy. Mol Cancer *19*, 120.

Zou, G. M., and Hu, W. Y. (2005). LIGHT regulates CD86 expression on dendritic cells through NF-kappaB, but not JNK/AP-1 signal transduction pathway. J Cell Physiol *205*, 437-443.

654 **Figure 1.** (A) Overall and disease-free Kaplan-Meier survival plots of PDAC patients segregated
655 into high or low CCL5 gene expression levels within pancreatic tumors. Data are derived from
656 CTPAC3 and TCGA cohorts and optimal cut-off values were calculated using the max-stat
657 method for each respective cohort. (B) Schematic overview of CCL5-responsive immune cells
658 and corresponding CCL5 receptor repertoire expression. (C) Correlation between overall and
659 single cell gene signatures of CCL5-responsive immune cells with overall PDAC prognosis.
660 Colour depicts positive (green), negative (red) or neutral (black) prognostic outcomes
661 (*p<0.05, ** p<0.01, *** p<0.005) . Data are derived from the Pathology Dataset of the
662 Human Protein Atlas19 and based on human tissue micro arrays and correlated log-rank p
663 value for Kaplan Meier analysis.
664 **Figure 2.** (A) Three different lineages of KPC pancreatic tumor cells (derived from
665 KrasG12Dp53R172HPdx1-Cre mice) were obtained and stained for DAPI (blue; nucleus), E-
666 cadherin (green; epithelial) and Vimentin (red; mesenchymal). Growth curve of orthotopically
667 injected KPC-F cells (500 cells) into the pancreas of wildtype C57BL/6 over time in weeks.
668 Tumor volume was measured using MRI. Representative MRI images over time are displayed,
669 white arrow denotes tumor mass. (B) Timeline of maraviroc (anti-CCR5) treatment regimen.
670 A total of 12 days post-orthotopic injection, tumor-bearing mice were treated daily with
671 maraviroc (10 mg/kg via intraperitoneal injection) for 6 days and followed for up to 30 days
672 after starting treatment. Frequencies of pancreatic tumor-infiltrating immune cells harvested
673 at day 30 with or without maraviroc using Aurora Cytek spectral flow is shown. Data are
674 represented as mean percentage positive cells (of CD45) ± SD. Significance was tested using
675 the Welch and Brown-Forsythe ANOVA for parametric data or Kruskal-Wallis test for non-
676 parametric data. Mock (n=6), IR (n=3), aPD1 (n=8), aPD1+IR (n=8), CCR5i (n=3), CCR5i+IR
677 (n=8), aPD1+CCR5i (n=5), aPD1+CCR5i+IR (n=8).
678 **Figure 3.** (A) Timeline of triple treatment regimen (maraviroc, αPD1 and radiotherapy)
679 following orthotopic injection of KPC_F cells. A total of 12 days post orthotopic injection of
680 500 KPC-F cells in the pancreas of wildtype C57BL/6 mice, mice were treated as follows:
681 seven consecutive days of 10 mg/kg intraperitoneal injection of maraviroc and four
682 alternating days of 10 mg/kg intraperitoneal injection of αPD1. Mice were followed for up to
683 30 days following the start of the treatment regimen. Tumor volumes were measured by MRI
684 and growth curves of individual treatment groups are plotted with or without radiotherapy as
685 measured by MRI. Average growth curves ± SD are depicted in bold, individual mice are

shaded (without IR; dashed, with IR; solid). Insert: expanded view of triple combination to show 'responders' display a significant benefit over RT alone. (B) Quantification of pancreatic tumors derived from (A) stained by IHC for p53. (C) Quantification of necrotic areas in pancreatic tumors derived from (A) based on H&E staining. (D) Quantification of infiltrating CD8+ in pancreatic tumors derived from (A) by flow cytometry. (E) Profiling of infiltrating immune cells in pancreatic tumors derived from (A) by Aurora Cytek as in figure 2B. Single, live cells were included for analysis and are represented as frequencies of CD45+ cells or total CD3+ for Foxp3+ Tregs. Significance was tested using the Welch and Brown-Forsythe ANOVA for parametric data # $p<0.05$, ##$p<0.01$ or Kruskal-Wallis test for non-parametric data #w $p<0.01$; pairwise comparisons (student t test) *$p<0.05$, **$p<0.01$, ***$p<0.005$, ****$p<0.001$.

Figure 4. (A) Spatial plots of individual cells identified using HALO software of scanned multiplex immunofluorescence murine pancreatic tumor slices. Positive staining is identified as the marker of interest and DAPI+ signal. Responders and non-responders to treatment are based on loss of E-cadherin staining. (B) Percentages of total DAPI+ immune cells (left) and E-cadherin+ tumor cells (right) derived from Figure 4A following treatment. Significance was tested using two-way ANOVA with Tukey multiple comparison (blue significance lines), or one-way ANOVA with Tukey multiple comparison (yellow significance lines) using a $p<0.05$. Correlations between %positive immune cells plotted against %positive E-cadherin+ cells, as derived from (A). Symbols and colours represent different treatment groups. (C) Correlation of total CD4 T (CD3+CD8-), CD8 T (CD3+CD8+) and NK cells (CD3-NK1.1+) plotted against %positive E-cadherin+ cells as derived from (A). (D) Correlation of %positive segregated NK cells plotted against %positive E-cadherin+ cells as derived from (A). NK cells were segregated based on expression of NKG2D; NKActive; NK1.1+NKG2D+; NKNKG2D-ve; NK1.1+NKG2D-. (E) Intratumoral immune cells of stratified pancreatic tumors based on low or high E-cadherin percentage (cut-off: 20%). Significance was tested for $p<0.05$ with a two-tailed student's T-test. * censored non-responder.

Figure 5. (A) UMAP of the CD8+ T and NK sub-clusters from Steele et al (arrows illustrate the developmental path of NK cells). (B) Dot plot showing the expression of exhaustion-related genes across CD8+ T and NK sub-clusters. (C) Dot plot showing highly expressed genes for each sub-cluster. (D) UMAP of the three NK subclusters (left), and violin plots comparing the expression of NK subtype-associated genes between the sub-clusters (right). (E) Dot plot

showing the different gene expression programs across the three NK sub-clusters. (F) Heatmap showing the top 15 upregulated markers for each NK sub-cluster.

Figure 6. (A) UMAP of the dendritic cell sub-clusters from the Steele dataset. (B) Violin plot showing the expression of XCL1, XCL2, and XCR1 across all cell types. (C) Circle plots showing interactions across all cell types (top left), signals coming from the tissue-resident NK cells (top right), the XCL1-XCR1 interaction (bottom left), and the XCL2-XCR1 interaction (bottom right). The width of edges represents the communication strength. (D) Heatmap showing the summary of secreted signalling communications of outgoing (left) and incoming (right) signals. The colour bar represents the communication strength, and the size of the bars represents the sum of signalling strength for each pathway or cell type. (E) Schematic overview of the trNK to cDC1 and cDC1 to CD8 T cell communication axis (top). Circle plots of all outgoing signals from cDC1 (bottom left) and the CXCL16-CXCR6 signalling (bottom right). (F) Correlation of HALO data on total NKNKG2D-ve/trNK cells (CD3-NK1.1+NKG2D-) with CD8 T (CD3+CD8+) from stained sections of treated KPC_F orthotopic tumors, R2 and p values indicate positive correlation across all tumors (gray, n=15) or limited to mock, CCR5i IR and CCR5i aPD1 IR combination (red, n =9). (G) Correlation of trNK signature with CD8A (left) or CD8B (right) in bulk RNAseq from TCGA_PAAD and binned into quartiles based on extent of cDC1 involvement as assume by cDC1 signature.

Figure 7. (A) Overall survival analysis correlating CD56 low/high expression with and without radiation therapy in the TCGA dataset. (B) Overall survival analysis correlating the deconvoluted NK C1 signature split into low and high. (C) Overall survival analysis correlating NK C1 low/high enrichment with and without radiation therapy in the TCGA dataset. (D) Boxplot correlating low and high CCL5 expression with NK C1 enrichment score in the TCGA (left) and CPTAC (right) datasets. (E) Overall (left) and disease-free survival (right) analysis of CCL5high patients segregated based on high/low enrichment of trNK (NK_C1) gene signature. (F) Overall survival of CCL5high segregated on CD56 (NCAM1) expression.

Figure 8. Correlation of tissue-resident NK cells gene signature in human cancer

The trNK cell gene signature is a positive prognostic factor across various malignancies using the TCGA_PAAD dataset.

Figure 1

A

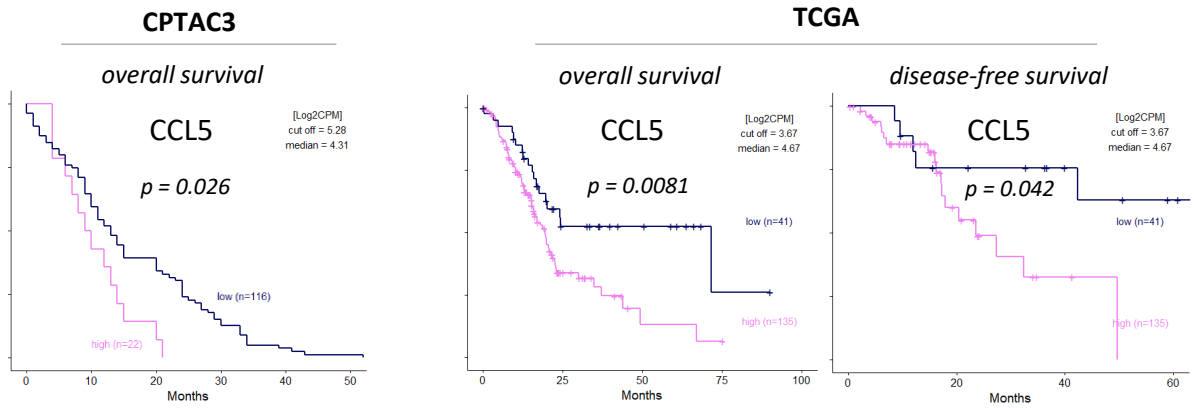

B

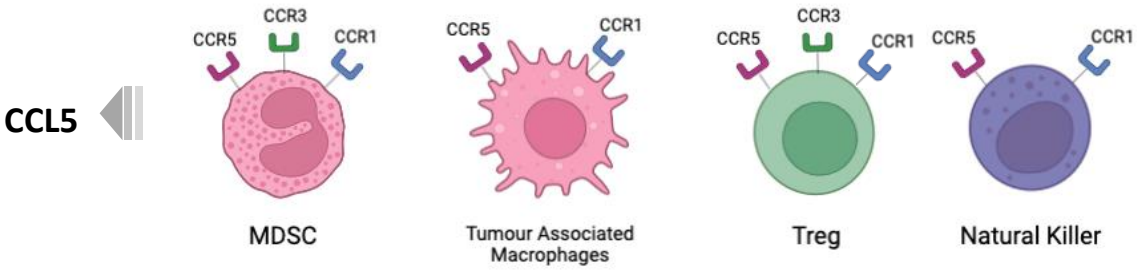

C

Human SCS signature genes

G-MDSC	p-value	M-MDSC	p-value	TAMs	p-value	Treg	p-value	NK	p-value
G-MDSC SCS sig	ns	M-MDSC SCS sig	ns	TAM SCS sig	ns	Treg SCS sig	ns	NK SCS sig	ns
S100P	0.0002	PLBD1	0.00017	MMP12	***	IKZF2	*	GZMB	*
IFITM2	***	VCAN	***	CD80	*	BLIMP1	*	PRF1	*
RNF24	**	SLC2A3	**	IL1β	*	CTLA4	ns	CD16	*
MME	**	S100A8	*	CCL13	*	TIGIT	ns	KIR	ns
CXCR2	ns	CSF3R	ns	APOE	ns	GITR	ns	NKG2A	ns
LIMK2	ns	FCN1	ns	IL12RB1	ns	BATF	ns	SELL	ns
GCA	ns	LYZ	ns	FLI1	*	IL2RA	ns	NKG2D	*
XPO6	ns	SELL	ns	SEPP1	*	FOXP3	**	CCR7	*
ARG2	***	ARG2	***	GPX3	**	BACH2	***	CD56	0.0000091

Figure 2

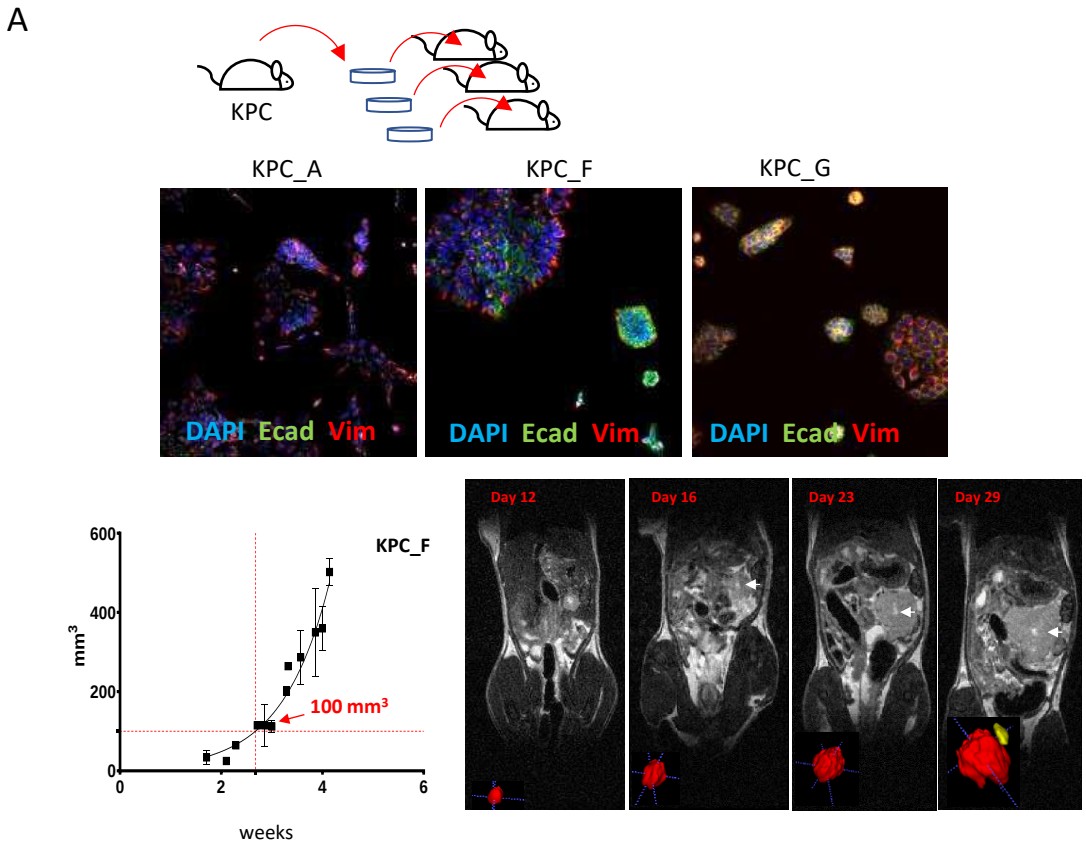

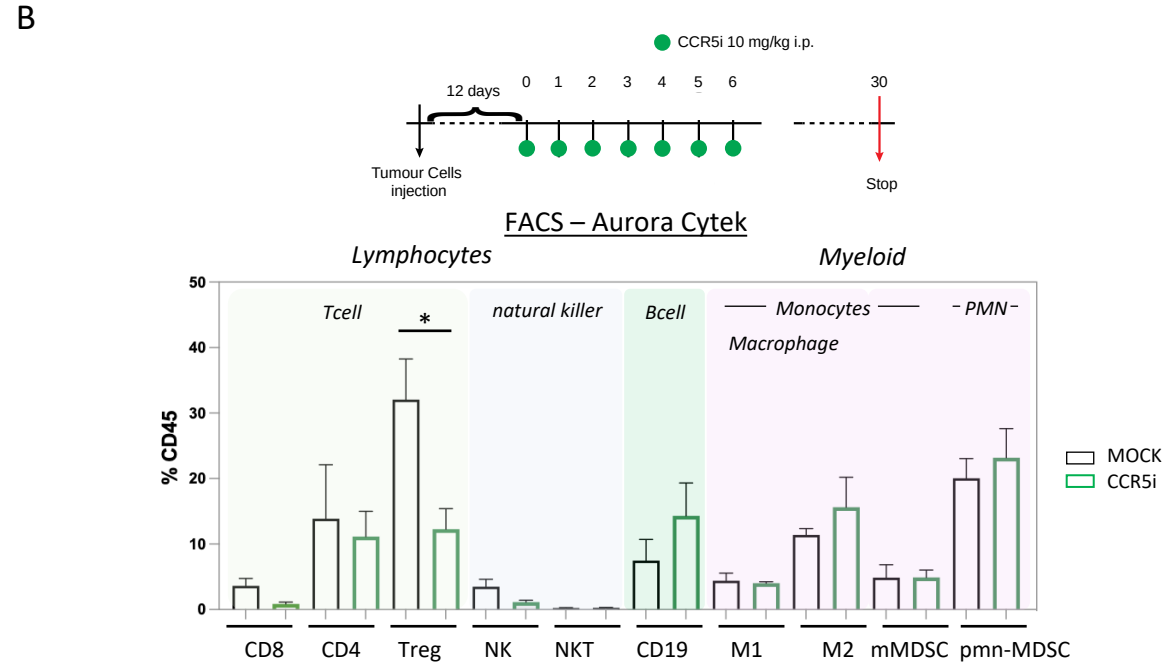

Figure 3

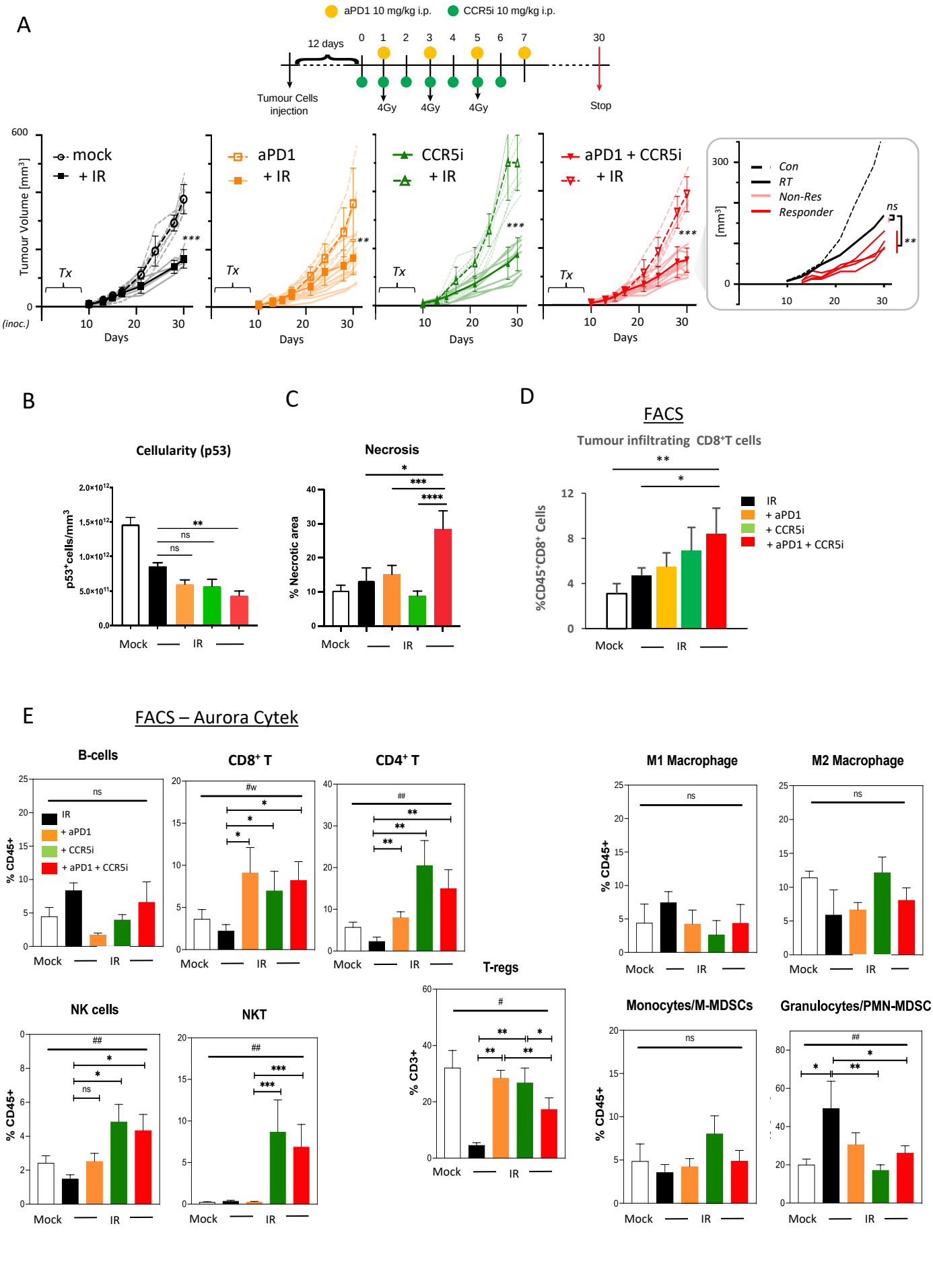

Figure 4

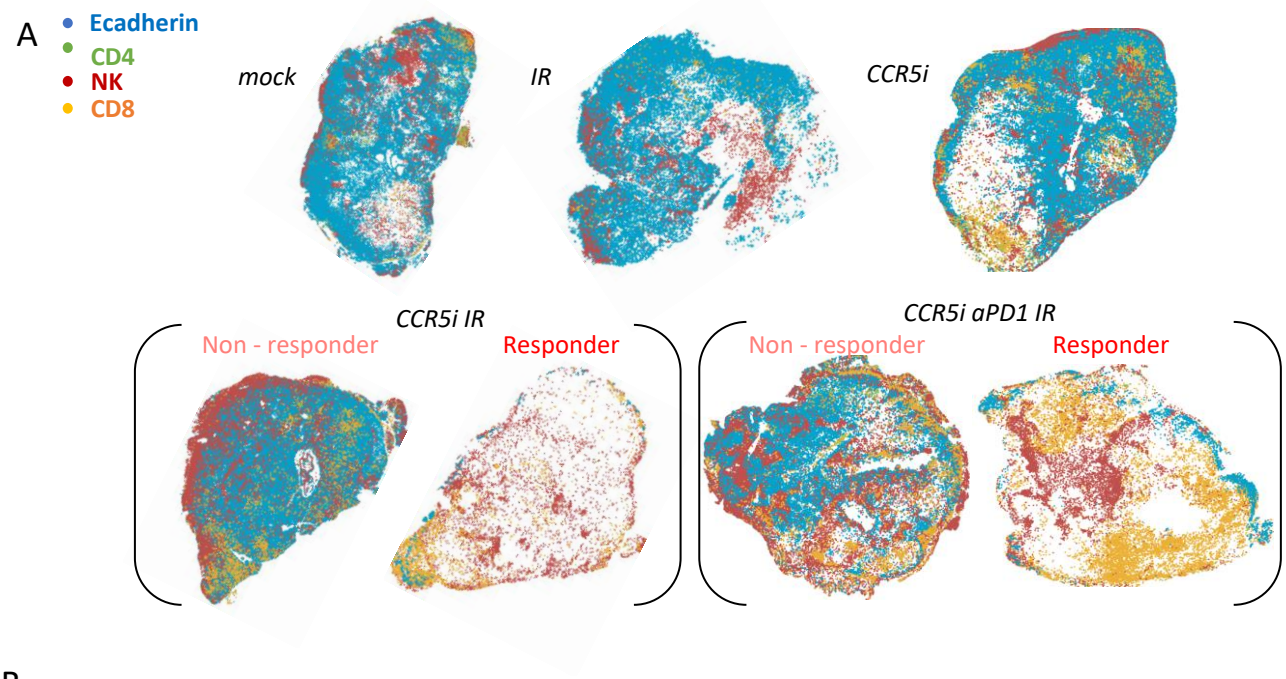

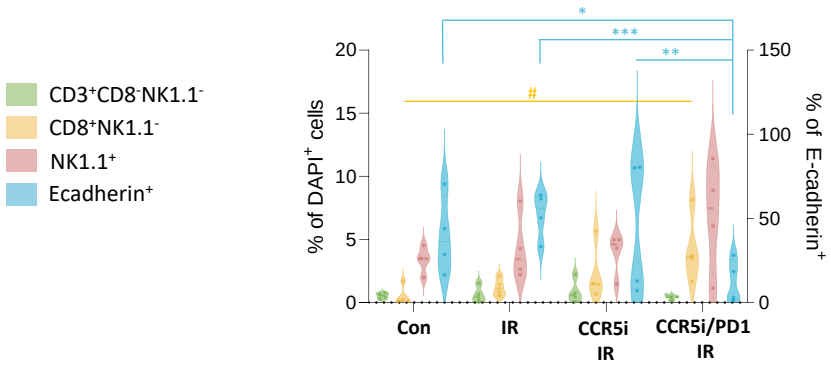

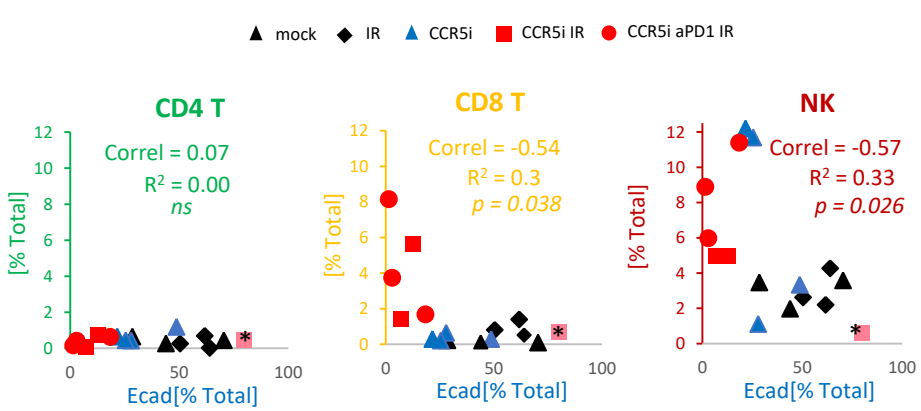

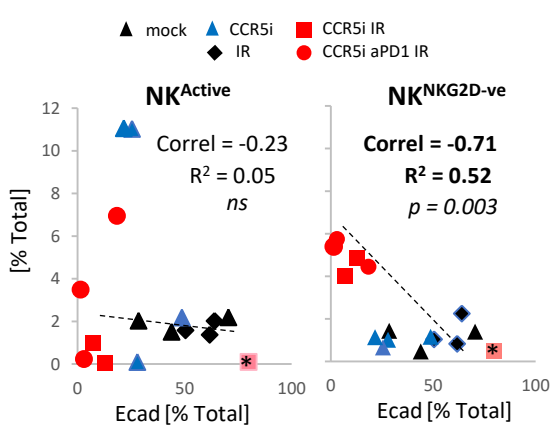

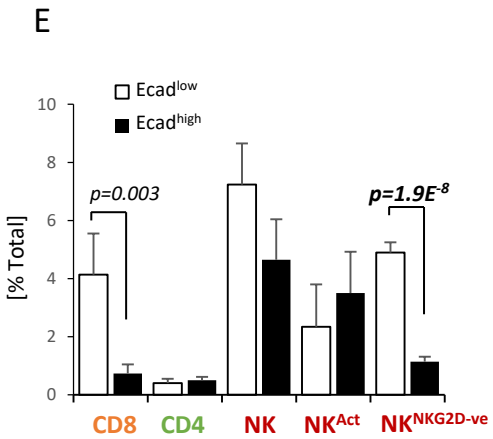

Figure 5

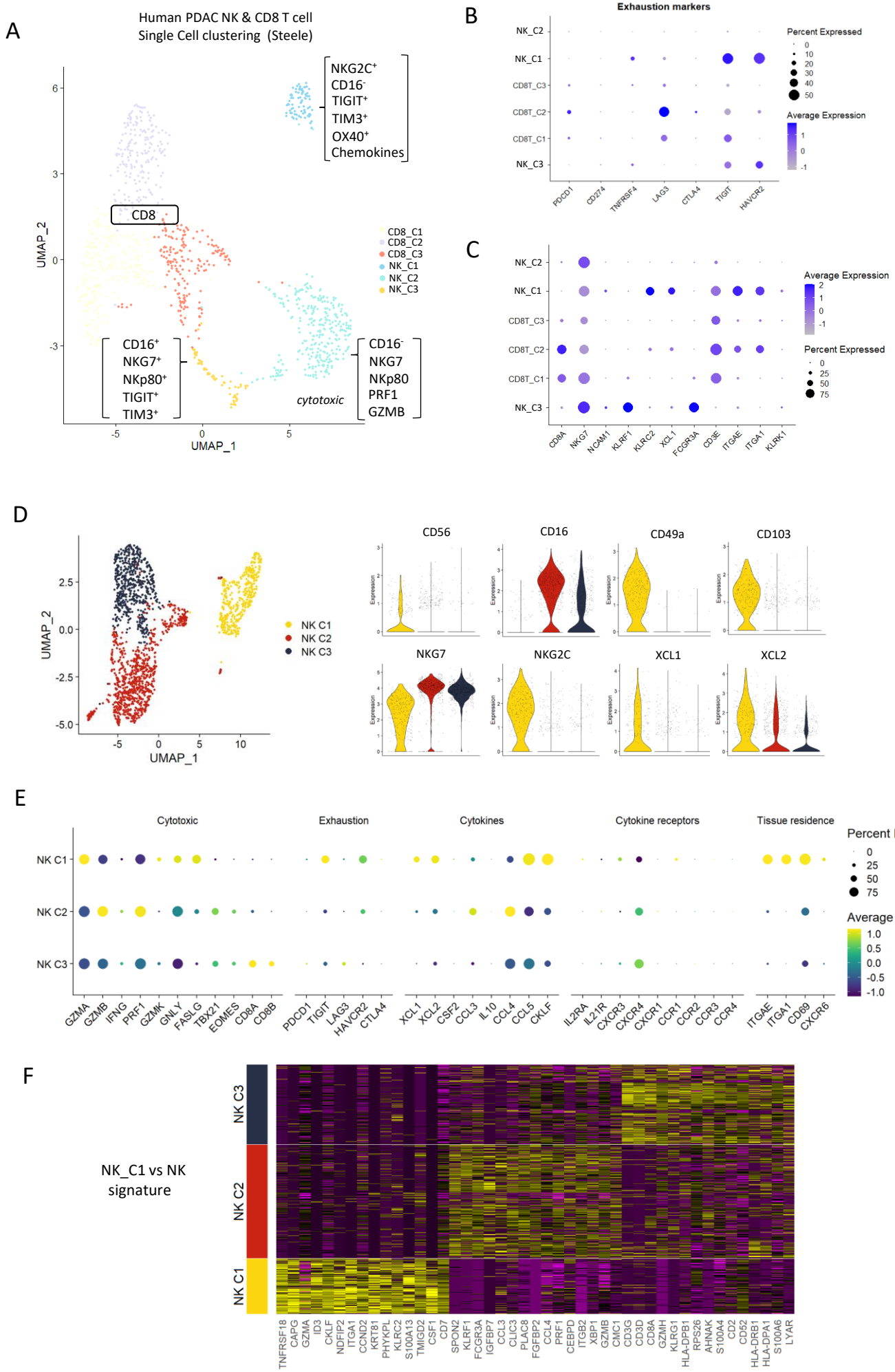

Figure 6

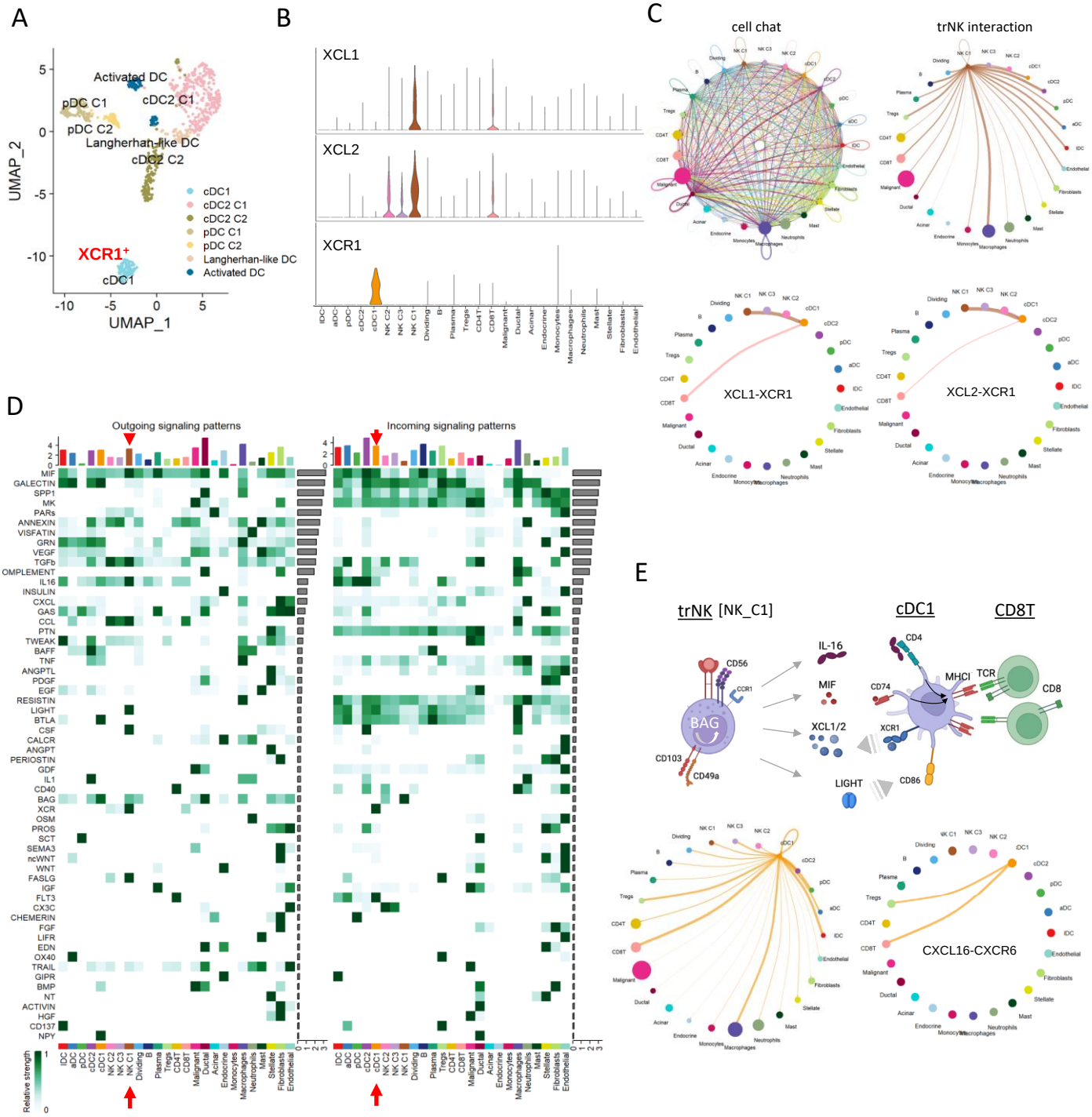

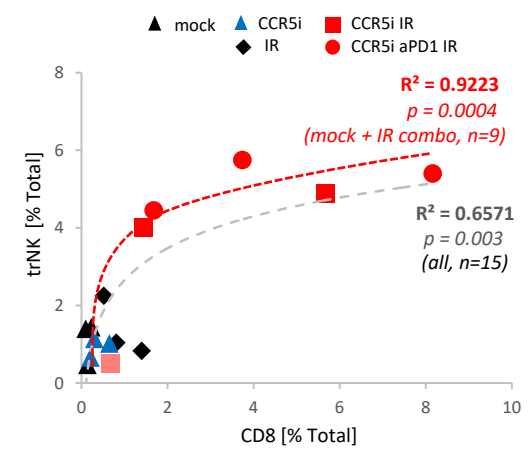

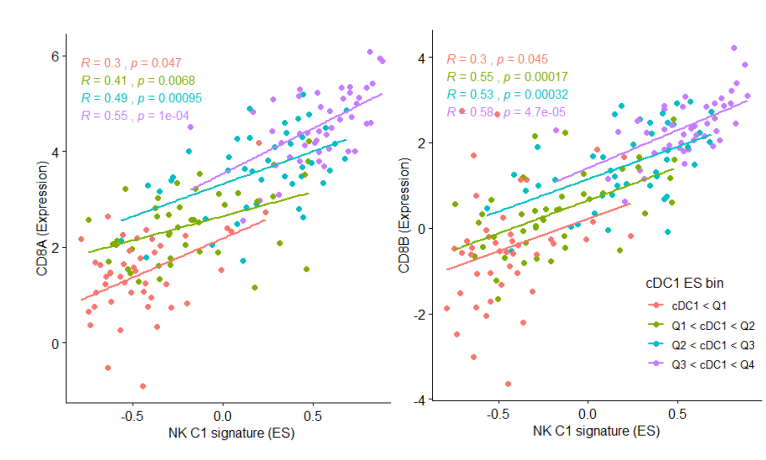

Figure 7

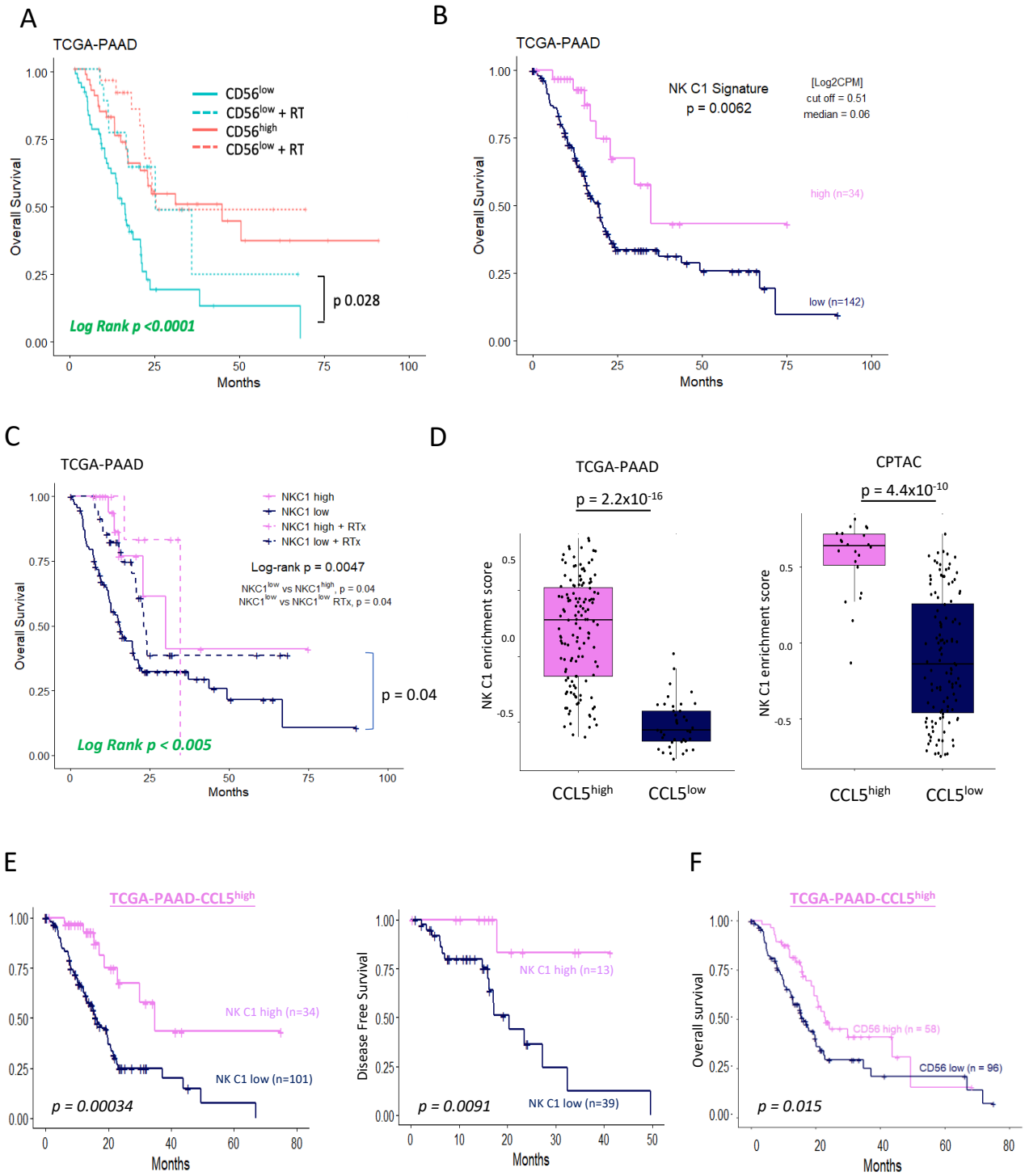

Figure 8